



Experimental Investigations On Self Compacting Concrete With Stainless Steel Slag As A Cementitious Material

**Dr.J.Anita Jessie¹, Dr.K.K.Gaayathri², Tarun Kumar Narnaure³, Devendra Dohare⁴,
Mohammad Parvej Alam⁵, Swapnil Balkrishna Gorade⁶**

¹Assistant Professor, Department of Civil Engineering, Vel Tech Rangarajan Dr.Sagunthala R&D Institute of Science and Technology, Avadi, Chennai, India.

²Assistant Professor, Department of Civil Engineering, Vel Tech Rangarajan Dr.Sagunthala R&D Institute of Science and Technology, Avadi, Chennai, India.

³Assistant Professor, Department of Civil Engineering and Applied Mechanics, Shri G. S. Institute of Technology and Science, 23 Sir M. Visvesvaraya Marg, Indore, Madhya Pradesh-452003, India.

⁴Associate Professor, Department of Civil Engineering and Applied Mechanics, Shri G. S. Institute of Technology and Science, Indore, Madhya Pradesh, India.

⁵Assistant Professor, Department of Civil Engineering, Shri Shankaracharya Institute of Professional Management and Technology, Mujgahan Sejabahar, Raipur, Chhattisgarh-492015, India.

⁶Assistant professor, Department of Civil Engineering, Pimpri Chinchwad College of Engineering, Nigdi, Pune, Maharashtra, India.

Article History: Received: 28.05.2023

Revised: 19.06.2023

Accepted: 17.07.2023

Abstract: Self-compacting concrete (SCC) with a 50% cement decrease is developed in this work. The feasibility of employing an alkali-activated blend of stainless steel slag (SSS) and fly ash (FA) as an alternative binder to cement has been established. SSS was processed using three distinct techniques. 35% SSS and 65% FA were used as precursors in the production of the binders, along with a hydroxide activating solution. For the creation of SCC, the 50% cement was used in place of this binder. The outcomes demonstrate high mechanical qualities and durability. The study demonstrates a decrease in cement consumption in the production of SCC by utilising two waste materials.

Keywords: stainless steel slag; alternative alkaline activation; self-compacting concrete; mechanical behaviour; durability properties.

DOI:10.48047/ecb/2023.12.10.459

1. Introduction

Over many years, improvements in research have been made in the hunt for novel materials with improved properties, more affordable manufacturing methods, and less pollution. Finding alternatives for ordinary Portland cement (OPC), the most used construction material, is a problem for these study areas. Expected are geopolymers the future's preferred cementitious material. Because of their qualities, they can be used as a whole or partial replacement for cement. Within the typology of alkaline-activated cementitious materials, geopolymers

constitute a subset. As an alternative to OPC, these materials exhibit unique features and functionalities that reduce the use of energy, natural resources, and CO₂ emissions [1].

Geopolymers have been created in recent years as a material to stabilise solid, hazardous, and radioactive waste. Geopolymers also possess cementitious qualities that are equivalent to OPC's. Due of the decreased CO₂ emissions (up to 80% less) during their manufacturing, they are viewed as an alternative to OPC [8,9]. Additionally, they demonstrate benefits in the mechanical characteristics and toughness of the created material [10,11], including strong resistance to acidic environments and freeze-thaw cycles, low permeability [12], and simple adhesion in glass, ceramic materials, concrete, and steel.

Several studies are investigating various by-products as potential precursors and activators in the creation of alkali-activated binders as a replacement for OPC in order to further knowledge and produce new raw materials [13]. Some of these substitutes, referred to as supplemental cementitious materials (SCMs), can be utilised to partially or entirely replace OPC in the manufacturing of concrete [14]. It has been established that silicates are required for the proper alkaline activation of a material. Studies for the substitution of synthetic alkaline silicates with waste high in silica have been developed recently. Ash from agroindustrial waste, such as rice husk ashes, sugar cane straw ashes, or biomass ashes, is one of the principal wastes thought to be a source of silica. Various researchers have researched all of these ashes, and it has been shown that they include crucial chemical components for cementing materials including silicon, aluminium, and sodium/potassium [15–20].

Several metallurgical operations have also been explored among the various waste materials, largely because of their amorphous shape, which offers them reactive hydraulic qualities, despite the fact that many studies have concentrated on the utilisation of ashes from various industrial activities. Positive findings were found for the compressive strength of geopolymers produced from metallurgical slag. SCMs are one type of metallic waste, along with the following: Iron, calcium, aluminium, silicon, and zinc are all present as oxides in zinc slag. Mixtures with compressive strengths of more than 50 MPa at 7 days and more than 70 MPa at 180 days were made possible by adding zinc slag to the geopolymer binder [21].

With a majority composition of SiO₂ (52.3%) and MgO (29.6%), nickel and magnesium slag was another type of metallurgical slag previously examined by other authors. When combined with coal fly ash, this slag produced geopolymers with a compressive strength of 60 MPa [22]. Smelting slag, which has a high concentration of iron silicates and a low CaO content, was another sort of waste from the metallurgical industry that researchers looked at. The compressive strength of this morphological feature decreased [23]. Ladle furnace slag and electric arc furnace slag investigations of alkaline activation of metallurgical wastes are the most prevalent. There aren't many studies on the subject of making concrete with activated steel slag. The majority of research focuses on using this waste in place of aggregates for making concrete.

Our analysis of the waste from one of the most active industrial areas, stainless steel slag (SSS), was prompted by the findings related to the activation of metallurgical waste. An innovative usage of activated stainless steel slag was made in this study to use cement and limestone filler instead of aggregates for making self-compacting concrete (SCC). In addition to having demonstrated (in earlier research) its feasibility for use as a cement alternative, the chemical characteristics of SSS also exhibit an activation potential, leading to improved mechanical behaviour. In this work, we assessed the effectiveness of fly ash (FA) and SSS alkaline activation for partial OPC replacement in concrete production. To assess how the pretreatments, SSS percentages, and curing circumstances affected the binder's mechanical behaviour, these

factors were evaluated. A fresh research was then conducted, in which the mixes that produced the greatest outcomes were utilised to make SCC instead of OPC and filler. As a result, the cement content of the alkali-activated SCC was reduced by as much as 50%.

2. Experimental Programme

In order to determine SSS's potential for alkaline activation and usage in the production of SCC as an OPC and filler alternative, this study tested it under various conditions.

The study was done in two steps. In the first stage, the potential for alkaline activation of SSS in the production of binders was assessed. Based on the findings of the mechanical behaviour, the best substitution ratios and treatments were chosen, and the chosen mixtures were then used in the production of SCC (Figure 1). To find the ideal ratio, geopolymer pastes with various SSS and FA doses were created, and the pastes were tested under various curing circumstances. An 8 molar activating solution of NaOH was used. A investigation of the compressive and flexural strengths of the produced pastes was done in order to evaluate the potential activation. After the geopolymer binder was evaluated, a research was conducted on the inclusion of binders with the ideal dose of SSS-FA as a cement alternative and filler in the production of SCC. Analysis was done on the alkali-activated SCC's mechanical behaviour.

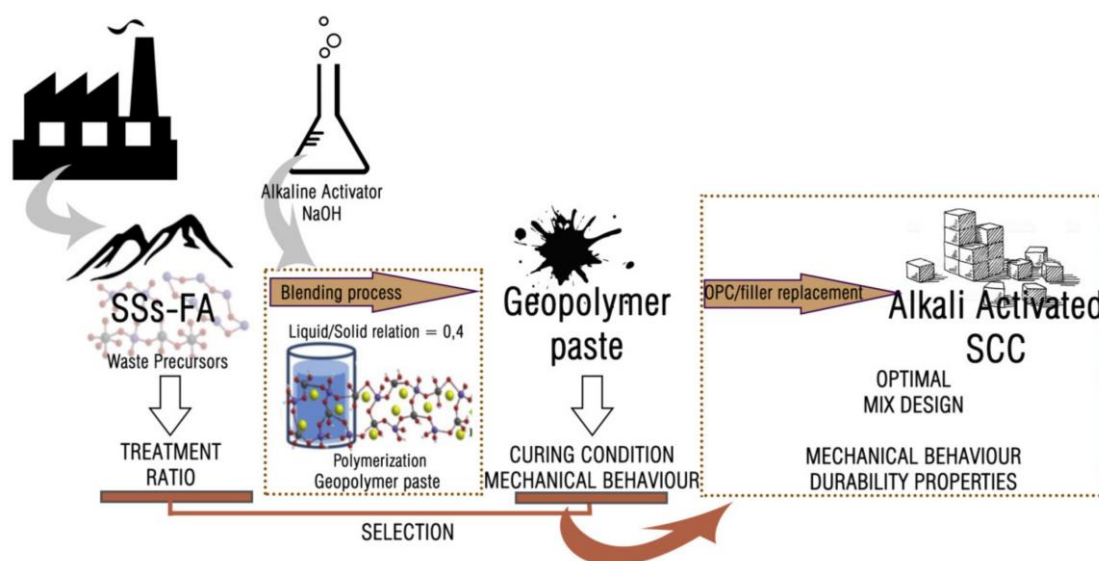


Figure 1. Diagram of the experimental methodology.

2.1. Materials

The stainless steel slag (SSS) was subjected to four different SSS processing methods in the current study: non-processed (SSS-NP), crushed and sieved SSS evaluated to obtain the fraction 0/125 m (SSS-C), SSS burned at a temperature of 800 C for 18 hours (SSS-B), and SSS-CB (stainless steel slag with combined crushing and burning treatment). The supplier of the stainless steel slag (SSS) was Acerinox Europa S.A.U., with offices in Los Barrios (Cádiz), Spain. CaO and SiO₂ were present in significant concentrations in SSS-NP, at 49.09% and 28.3%, respectively. Despite minor differences in the CaO, SiO₂, and MgO concentrations, the compositions of SSS-C, SSS-B, and SSS-CB were comparable. In comparison to SSS-NP, the proportions of these components were greater. Additionally, the density and water absorption were reduced by the SSS treatment. Regarding the characteristics of FA, all SSS samples

displayed greater values for density and absorption along with rising CaO and MgO values. In contrast, SiO₂ and Al₂O₃ levels in the SSS were lower than those in the FA. SSS has a high oxide concentration, including CaO, SiO₂, and MgO, which indicates that it has a chemical potential that can be triggered.

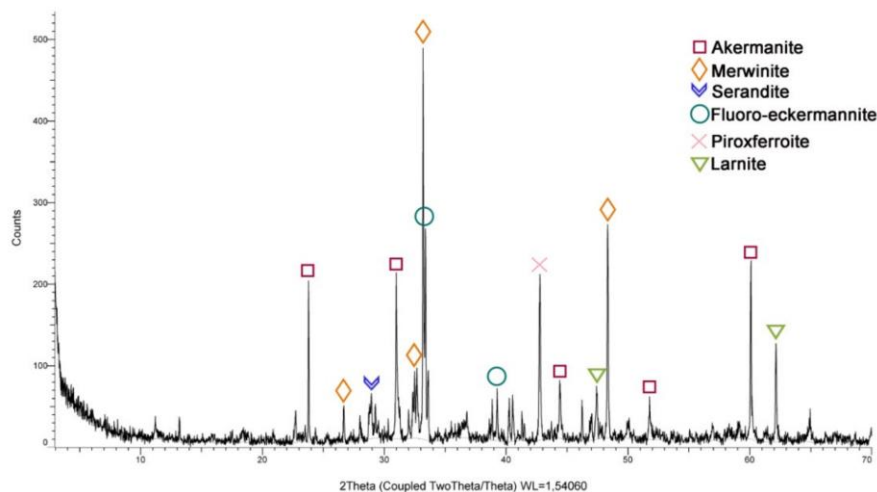


Figure 2. SSS diffractogram—XRD.

Merwinite ($\text{Ca}_3\text{Mg}(\text{SiO}_4)_2$), calcium-magnesiumsilica oxide, and akermanite (Ca-Mg-Si) made up the majority of the SSS's mineral makeup. The elemental components in Table 1 and this mineralogy are equivalent. A high SiO₂ concentration distinguishes the natural pozzolans used in the production of cement. A strong pozzolanic activity in cements is implied by a high SiO₂ concentration of natural pozzolan. The pozzolanic activity of materials was traditionally determined in accordance with certain restrictions in their chemical composition. Figure 3 compares the chemical composition of FA and SSS to the acceptable values for pozzolanic materials.

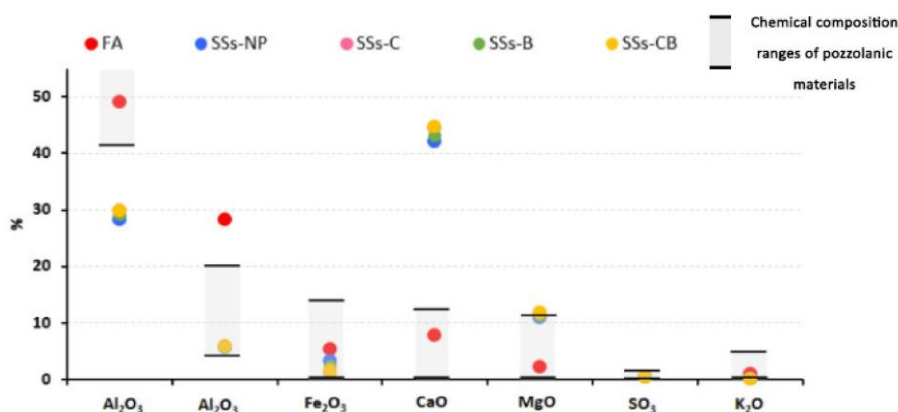


Figure 3. Chemical composition of FA and SSS in relation to ranges established for pozzolanic materials.

However, SSS with all treatments done was revealed to be beyond these limitations, having lower amounts of SiO₂ and greater values of CaO than standard pozzolans. It can be shown that FA is within the limits defined for SiO₂ and CaO. Ash with a high calcium concentration exhibits pozzolanic and hydraulic behaviour, according to recent investigations. As a result, the high CaO levels seen in SSS would enable its alkaline activation, producing a substance with

cementing activity. A pozzolanicity analysis was conducted on each of the materials in line with the UNE-EN 196-5:2011 standard to confirm this pozzolanic activity.

Figure 4 displays the $[\text{OH}]$ vs. $[\text{CaO}]$ diagram with the Frattini test findings at 8 and 14 days put on it.

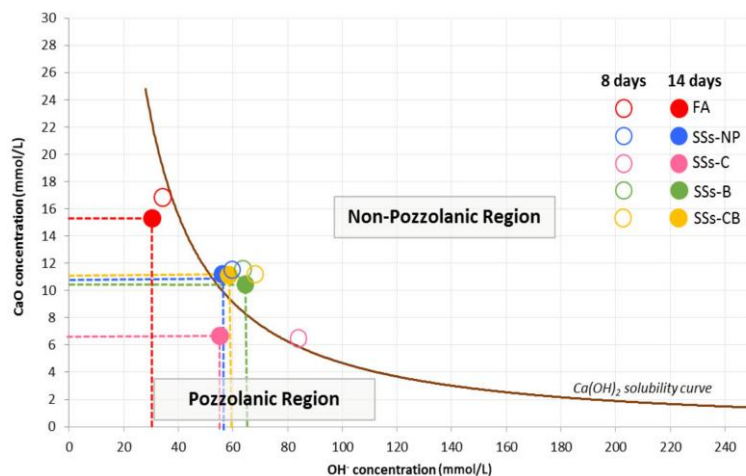


Figure 4. Result of Frattini test at 8 and 14 days of FA and SSS.

At 8 and 14 days, SSS with various treatments administered demonstrated negative pozzolanicity. However, after 14 days, the use of a crushing therapy (SSS-C) revealed good pozzolanicity. According to Frattini's test, Figure 1's results on the change of $[\text{OH}]$ and $[\text{CaO}]$ demonstrate that SSS-C has a high level of pozzolanic activity whereas SSS-NP, SSS-B, SSS-CB, and FA have lower levels. SSS-C revealed low $[\text{OH}]$ and $[\text{CaO}]$ values, placing this slag in the Frattini-described "pozzolanic region" (Figure 4). The remaining slags that were examined have higher $[\text{OH}]$ and $[\text{CaO}]$ concentration values, which position them in the "non-pozzolanic region" with a reduced activation potential.

According to earlier research, SSS behave in a manner consistent with pathway B, which was identified by Pourkhorshidi et al. as the mechanism used by highly active pozzolans. SSS and FA have a similar reaction trajectory in the pozzolanicity assessment diagram (Figure 4), where the values decrease in alkalinity and Ca ion concentration over time. Pozzolans, such as fly ash or silica fume, are to blame for this conduct.

2.2. Mix Proportions and Manufacture of Geopolymer Pastes SSS-FA and Alkali-Activated Self-Compacting Concrete

Various binder combinations were created in order to examine the potential activation. An earlier investigation looked at whether the SSS might be activated by using NaOH 8 molar.

In order to ensure similar, uniform values were employed throughout all of the binder mixes, a liquid/solid ratio of 0.4 was used in each mixture. Two series were conducted using two different curing conditions and each processed SSS (70%SSS-30%FA and 35%SSS-65%FA) (Figure 5).



Figure 5. Alkali-activated SSS-FA pastes.

Two sets of curing conditions were used once the pastes were created. The pastes were first dried out and cured in a wet chamber at 20 C and 100% humidity after being baked at 40 C for 22 hours. Similar to the first technique, a second curing system was used; this time, the oven's beginning temperature was 80 C, and the remainder of the process was the same.

The right quantity of cement, water, and fine aggregates must be used to create classic SCC, taking into account the self-compacting properties of the material in proportion to its flowability. Powdered pozzolanic fillers, fluidisers, and additives are utilised because the water/cement ratio must be kept under control to prevent strength loss. In this work, an alkali-activated binder containing SSS-FA takes the place of the cement and limestone filler used to make conventional SCC. In order to create alkali-activated SCC, all of the limestone filler and 50% of the OPC were swapped out for the binder SSS-FA.

Additionally, the quantity of admixture needed to produce appropriate SCC flowability as well as the amount of NaOH solution utilised to alter the mixing water in each of the created mixes were taken into account.

Three series of alkali-activated SCC were created using the doses of the SSS-FA binder that produced the strongest effects. An evaluation control mix was created to assess the outcomes.

Eight different steps made up the SCC manufacturing process.

1. Making a binder by dissolving SSS-FA in NaOH
2. A cement-aggregate combination
3. Including a binder.
4. Add remaining water and the additive.
5. Flow extension test consistency measurement
6. Filling of specimens
7. Curing in an oven at 80 °C for 22 hours.
8. De-molding and preservation in the curing chamber.

3. Test Methods and Results

3.1. Flowability

A thorough investigation of consistency is related to the production of SCC [54]. In order to examine this attribute, three distinct techniques were used: the slump test in accordance with UNE-EN 12350-10:2011, the L-box in accordance with UNE-EN 12350-10:2011, and the J-ring in accordance with UNE-EN 12350-12:2011.

According to the three rules that were used, the data obtained demonstrated that all of the mixes were within the slump limitations defined for SCC. In comparison to the control SCC, flow values for SCC produced with SSS-FA activated binder increased.

Due to the spherical form of the FA in the active binder, which increases the volume of the paste and reduces friction in the mix, the consistency increases with the addition of the activated binder. To examine the flowability of SCC mixes, L-Box experiments were also carried out. Table 5 demonstrates that all combinations have a strong ability to flow through reinforcement bars without the use of equipment for compacting, as shown by the fact that all values of the H2/H1 blocking ratio fall within the standards' permissible range of 0.88 to 0.93.

Testing on J-Rings was also done. The measurements between the inside and outside of the J-Ring ranged from 3.9 to 5.1 mm, falling within the rules' set parameters. Regarding how SSS treatment affected the consistency of the activated SCC paste, it was found that applying crushing and burning enhanced slump flow. According to the results, all mixes showed to be appropriate for use on structural elements with reinforcement.

3.2. SSS-FA Binder—Compressive and Flexural Strength

An initial research of the flexural and compressive strength of pastes prepared with various percentages of SS and FA activated with NaOH and cured under two different circumstances was carried out in order to produce SSS-FA mixtures suitable for use as cement alternatives in the fabrication of SCC.

Under curing conditions at 80 °C, it can be shown that the findings for flexural and compressive strength increased (Table 6). The activation of SSS is better suited to the curing conditions at this temperature. Similar findings were made in earlier research [16], where it was found that pastes cured at 45 °C did not harden, but those cured at 80 °C could be withdrawn from the moulds and shown resistance to mechanical testing.

The pastes made with 100% FA showed the best results for compressive strength. Compressive strength dropped when SSS was added, reaching values of a loss of around 55-75% in pastes made with 70% SSS and 30% FA. Similar outcomes were found in other investigations [22] using different kinds of metallurgical slag. The researchers demonstrated that larger replacement levels, like 60%, appeared to have a detrimental effect on the strength growth in alkali-activated steel slag. Three mixtures of alkali-activated SSS-FA were chosen for the production of SSC in accordance with the results. The blends with the highest compressive strength after 28 days were chosen.

3.3. SCC—Compressive Strength

According to UNE-EN 12390-3, the compressive strength was assessed for three 100 mm cubic samples during 7 and 28 day periods.

The typology relates to a certain type of activation pattern (C-A-S-H), a material rich in calcium and silicon ($\text{SiO}_2 + \text{CaO} > 70\%$), as evidenced by the composition of the SSS (Table 1). Under rather mild alkaline conditions, it is activated.

At 28 days, the compressive strength of every series produced was greater than 30 MPa.

50% less cement is used when activated SSS is used. The loss of strength is correlated with this decline, although it was 19.19% in 35SSS-NP, 16.94% in 35SSS-C, and 16.39% in 35SSS-B.

In contrast to earlier investigations, where the use of NaOH-activated blast furnace slag led to a loss of strength of around 65% over a control concrete, the decline in compressive strength with the use of activated SSS as a cement replacement was smaller.

In comparison to a control, the relative strength loss in the application of SSS was substantially more in the pastes examined than in the produced SCC (Figure).

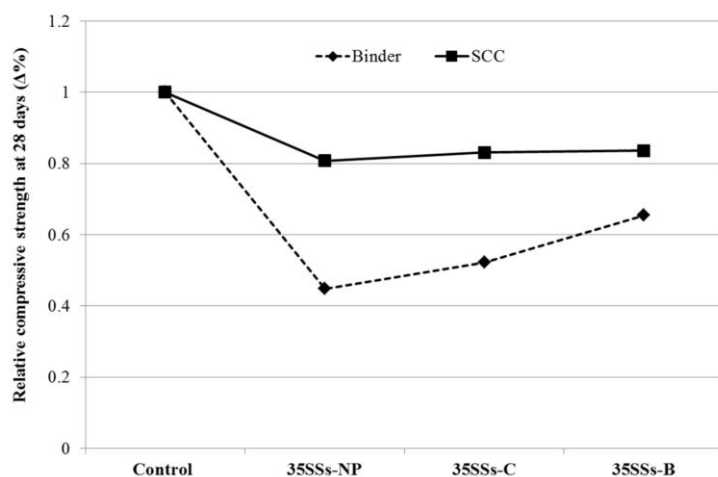


Figure 6. Relative compressive strength of binder and SCC at 28 days versus control.

3.4. SCC—Splitting Tensile Strength

An analysis of the SCC's tensile strength after 28 days was done. This feature depends on the quality and kind of connections formed between the employed aggregates and the cementitious matrix as well as any microcracks or other flaws in the matrix. It is not only dependent on the strength of the aggregates used.

The behaviour of concrete against the start and spread of fractures, the anchoring of steel reinforcement, or shearing is closely correlated with its tensile strength. The concrete's compressive strength may be used to forecast the tensile strength value. The tensile strength is predicted using the formulae presented in Eurocode 2. According to Equation (1), the compressive strength is calculated for both standards.

$$f_{ct,sp} = \frac{1}{3}(f_{cm} - 8 \text{ MPa})^{\frac{2}{3}} \quad (1)$$

The results for tensile strength are shown in Figure 7, along with a comparison to the compressive strength of alkali-activated SCC. Also displayed are the theoretical tensile strength values derived from Equation (1). In contrast to the results for compressive strength, all SCCs made with binder SSS-FA had greater tensile strength values than the control. The outcomes of control SCC might be anticipated by using the theoretical Equation (1). However, as the application of SSS resulted in a gain in tensile strength unrelated to compressive strength, it cannot be applied to alkali-activated SCC. SCC's tensile strength ratings rose when SSS was crushed and burned.

3.5. Water Absorption, Density, and Accessible Porosity

To determine the effects of using an alkali-activated SSS-FA binder to substitute cement and limestone filler in the hardened condition of the concrete, a research of the density, absorption, and porosity of SCC was conducted.

The apparent volume of the samples was initially calculated using a hydrostatic balance under saturation circumstances to get these concrete characteristics. The occluded air was then removed by placing them in a vacuum chamber for 24 hours. The specimens were remained immersed for a further 24 hours to ensure complete saturation after the pores were filled with water during the course of the following 24 hours by overpressure. This process was used to get the apparent volume and dry weight before being placed in an oven at 110 °C. The formulas outlined in the rules were then used to gather the data in order to determine the accessible porosity, apparent density, and absorption coefficient. Fly ash usage in concrete has been demonstrated to lower permeability metrics in prior research. The combined use of FA and SSS reduced porosity and absorption, a characteristic that is directly associated to superior durability performance, according to similar findings in this study.

In order to minimise the porosity of the concrete, activated SSS is used. This creates a gel that fills the pores and creates a denser microstructure. Previous investigations came to the conclusion that using an alkaline solution with more OH ions resulted in a decrease in permeability that was directly linked to better mechanical qualities.

3.6. Macroporosity through Digital Image Analysis

In various studies, image analysis has been utilised to characterise concrete, analyse its pore structure, and assess its permeability. The samples used for the image analysis were 100 mm cubic specimens with 50 mm slices. A white pigment was added after the surface was polished. Software for image processing and analysis (ImageJTM, Rasband W. A free Java image processing programme) was used to analyse the photos. Bethesda, Maryland: National Institute of Mental Health (2008.).

Figure 8 displays the digital pictures that have been processed to illustrate the distribution of pores in control and alkali-activated SCC. The sample that had the least porosity (35SSS-C) was the self-compacting concrete prepared using SSS-C.

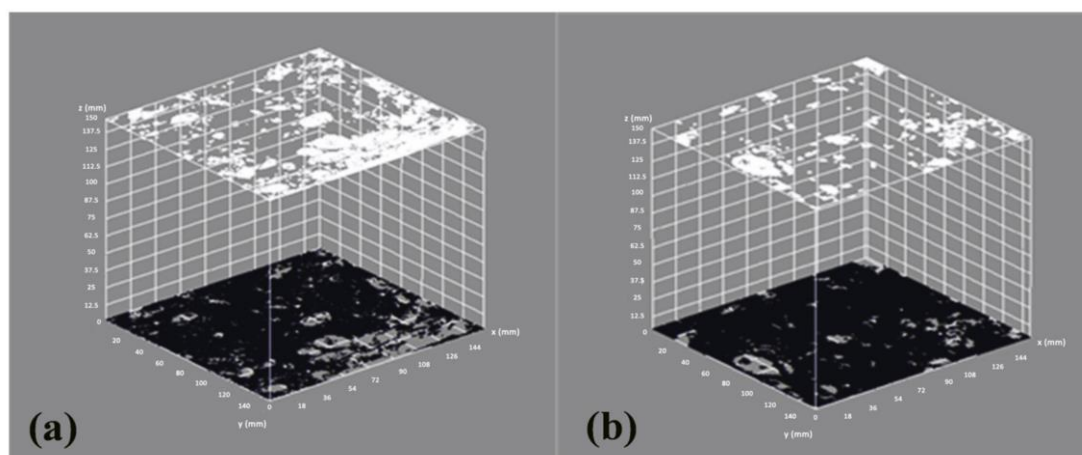


Figure 8. Pore structures of (a) SCC control and (b) 35SSS-C. Indicating in white the pores and in black the solid section.

According to image analysis, the SCC control had much more porosity than the SCC 35SSS-C made using an alkali-activated SSS binder. The holes in the 35SSS-NP samples were more numerous and distributed on the surface, whereas the pores in the control sample were bigger, more connected, and had a greater volume porosity. SSS has a lot of calcium, and the slags are what make up the binder, creating a tight and compact matrix that minimises the number of pores. This is partly because the gel generated in this situation is C-A-S-H rather than N-A-S-H. In alkali-activated SCC specimens with SSS, less open porosity is strongly correlated with higher tensile strength values.

3.7. Carbonation Depth

To assess the impact that too much humidity can have on the steel reinforcement utilised in SCC, a carbonation research is required. The SCC starts out with a fundamental character medium (pH 12). The steel reinforcement is passive in these circumstances and cannot be corroded. However, over time and as a result of the portlandite's interaction with the surrounding CO₂, this pH falls to levels below 9. In this case, the steel is no longer shielded from corrosion by the concrete, and if there is enough moisture, the corrosion will manifest as the accompanying lesions. The penetration of the carbonates was assessed using the UNE 112011:2011 technique.

Prismatic samples of 100 mm x 100 mm that had previously been cured for 28 days in a wet room were put in an accelerated carbonation chamber with 60% humidity, 23 °C, and 5% CO₂. For 1, 28, 56, and 90 days, carbonation depth was assessed. The pH shift was measured using an indicator that was atomized onto a sample break (1% phenolphthalein solution in alcohol). The carbonation coefficient was used to gauge the degree of carbonation. This variable is affected by the depth (Cd) in relation to the square root of the period in years (Figure 9).

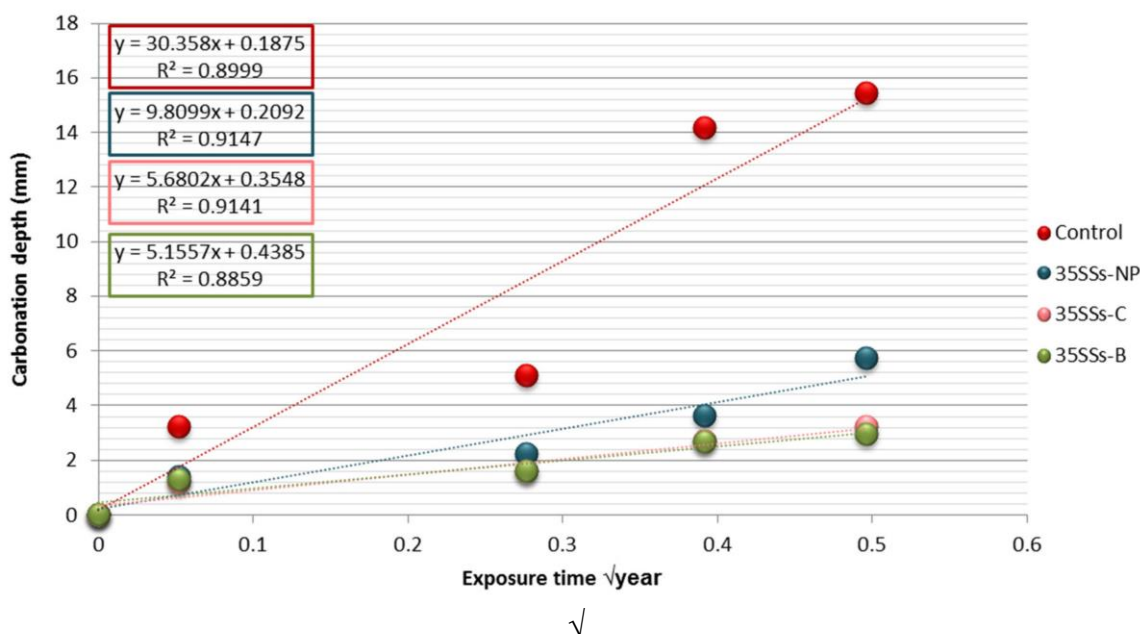


Figure 9. Carbonation depth according to t of SCC control, 35SSS-NP, 35SSS-C, and 35SSS-B.

All specimens created with the SSS-FA alkali-activated binder had lower carbonation depths than the control. When the SSS was exposed to crushing and burning procedures, less depth was seen. Figure 10 compares the 90-day carbonation depth in 35SSS-C specimens to that of SCC control specimens (Figure 10a). Figure 10b demonstrates how the carbonation depth of

the specimen was decreased by using alkali-activated SSS in the production of SCC as a cement replacement. The carbonation depth in the 35SSS-C specimen was less than 3 mm, whereas the SCC control revealed an outside carbonation perimeter of almost 15.5 mm.

The material's porosity has a significant role in regulating the degree of carbonation in SCC. The use of alkaline-activated SSS results in a reduction in the porosity of the material, as illustrated in Figure 8 and Table 8, in addition to a 50% reduction in cement content and a 100% reduction in limestone filler content. In contrast to the findings of other research, where the introduction of FA and steel slag resulted in an increase in porosity and depth of carbonation in SCC, the carbonation depth in these combinations is lower.

This study demonstrates that when SSS and FA are combined, both attributes are decreased. Along with the material's porosity, the high $\text{Ca}(\text{OH})_2$ concentration buffers the carbonation process by releasing hydroxide when the pH starts to fall. A reduced $\text{Ca}(\text{OH})_2$ concentration causes a decrease in alkalinity, which causes increased carbonation, worse mechanical performance, and the potential for reinforcement corrosion.

This demonstrates that using more alkali-activated binder in the mixes causes the carbonation depth to decrease. Figures 9 and 10 illustrate this outcome, where carbonation penetration was decreased by 70–85% in alkaline-activated SCC specimens compared to control SCC.

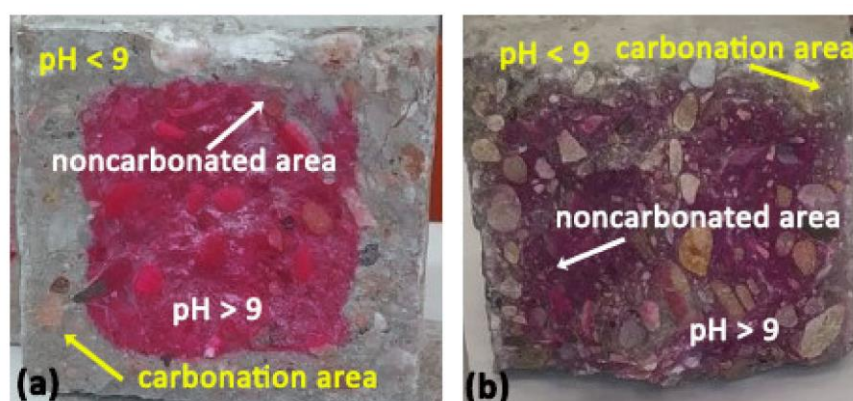


Figure 10. Transverse section of carbonated SCC specimens after 90 days of exposure: (a) SCC control and (b) 35SSS-C.

4. Conclusions

The idea of using alkali-activated SSS in place of Portland cement and limestone filler in the production of SCC has been explored by this study. It has assessed the effects of SSS treatment on its physical-chemical characteristics as well as the effects of its use on the alkali-activated SCC's mechanical qualities and durability. The results showed the following:

- The chemical composition presented by SS is appropriate for the possible alkali activation. SiO_2 , CaO , and MgO make up the majority of SSS. These three components are increased as a result of the use of crushing and burning treatments. Although they are mostly made of merwinite, calcium oxide, magnesium, silica, and akermanite (Ca-MgSi), and their mineralogy displays a crystalline structure that makes activation difficult, pozzolanicity tests showed the pozzolanic capability when a crushing.
- The strength of pastes made using SSS-FA and NaOH as an alkaline activator decreased as the amount of SSS rose in initial mechanical performance testing. It is crucial to note that the mechanical behaviour improves with the use of the proper curing conditions and various

SSS treatments. For the production of alkali-activated SCC, three ideal binder doses (35SSS-NP, 35SSS-C, and 35SSS-B) were discovered.

- The production of SCC with the replacement of 50% cement by a binder made with SSS and FA resulted in a 10–14% reduction in compressive strength. Indirect traction and compression tests produced better results when SSS was treated. The compressive strength of every series produced using SSS was better than 30 MPa. iv. When compared to a control SCC, SCC made with alkali-activated SSS considerably reduced porosity and absorption characteristics. When compared to conventional SCC specimens, alkaliactivated SCC specimens with SSS had lower pore volumes, according to imaging analysis used to assess macroporosity. A link to a lower pore was also visible. The amount of carbonation is closely correlated with the loss in porosity and higher pH of alkali-activated SCC. The carbonation depth was lowered by up to 85% when SCC was alkali-activated with SSS. Long-term effects of this component include increased mechanical performance and less corrosion of steel reinforcements often utilised in SCC.
- Finally, the use of the alkali-activated SSS binder in conjunction with FA and NaOH as an activator reveals the feasibility of 50% substitution of Portland cement and limestone filler in the production of SCC under specific curing conditions at 80 C for the first 22 hours.
- Although the values achieved surpass those required by standards, the use of alkali-activated SSS decreases compressive strength. In addition to having less cement, alkali-activated SCC performed better in terms of tensile behaviour, porosity, and carbonation penetration. This approach has a significant impact on lowering CO₂ emissions during the manufacture of Portland cement and long-term SCC strength.

References

1. Ammenberg, J.; Baas, L.; Eklund, M.; Feiz, R.; Helgstrand, A.; Marshall, R. Improving the CO₂ performance of cement, part III: The relevance of industrial symbiosis and how to measure its impact. *J. Clean. Prod.* **2015**, *98*, 145–155. [CrossRef]
2. Vance, E.; Perera, D. Geopolymers for nuclear waste immobilisation. In *Geopolymers*; Elsevier: Amsterdam, The Netherlands, 2009; pp. 401–420. [CrossRef]
3. Galiano, Y.L.; Pereira, C.F.; Vale, J. Stabilization/solidification of a municipal solid waste incineration residue using fly ash-based geopolymers. *J. Hazard. Mater.* **2011**, *185*, 373–381. [CrossRef] [PubMed]
4. Pereira, C.F.; Luna, Y.; Querol, X.; Antenucci, D.; Vale, J. Waste stabilization/solidification of an electric arc furnace dust using fly ash-based geopolymers. *Fuel* **2009**, *88*, 1185–1193. [CrossRef]
5. Lancellotti, I.; Kamseu, E.; Michelazzi, M.; Barbieri, L.; Corradi, A.; Leonelli, C. Chemical stability of geopolymers containing municipal solid waste incinerator fly ash. *Waste Manag.* **2010**, *30*, 673–679. [CrossRef] [PubMed]
6. Dassekpo, J.-B.M.; Ning, J.; Zha, X. Potential solidification/stabilization of clay-waste using green geopolymer remediation technologies. *Process Saf. Environ. Prot.* **2018**, *117*, 684–693. [CrossRef]
7. Shi, C.; Fernández-Jiménez, A. Stabilization/solidification of hazardous and radioactive wastes with alkali-activated cements. *J. Hazard. Mater.* **2006**, *137*, 1656–1663. [CrossRef]
8. Davidovits, J. Geopolymer cements to minimize carbon dioxide greenhouse warming. *Ceram. Trans.* **1993**, *37*, 165–182.
9. McLellan, B.C.; Williams, R.P.; Lay, J.; Van Riessen, A.; Corder, G.D. Costs and carbon emissions for geopolymer pastes in comparison to ordinary portland cement. *J. Clean. Prod.* **2011**, *19*, 1080–1090. [CrossRef]

10. Duxson, P.; Fernández-Jiménez, A.; Provis, J.L.; Lukey, G.C.; Palomo, A.; van Deventer, J.S. Geopolymer technology: The current state of the art. *J. Mater. Sci.* **2007**, *42*, 2917–2933. [CrossRef]
11. Kong, D.L.; Sanjayan, J.G. Effect of elevated temperatures on geopolymer paste, mortar and concrete. *Cem. Concr. Res.* **2010**, *40*, 334–339. [CrossRef]
12. Davidovits, J. Properties of geopolymer cements. In Proceedings of the First International Conference on Alkaline Cements and Concretes, Kiev, Ukraine, 11–14 October 1994; pp. 131–149.
13. Payá, J.; Agrelá, F.; Rosales, J.; Morales, M.M.; Borrachero, M.V. Application of alkali-activated industrial waste. In *New Trends in Eco-Efficient and Recycled Concrete*; Elsevier: Amsterdam, The Netherlands, 2019; pp. 357–424. [CrossRef]
14. Ishak, S.A.; Hashim, H. Low carbon measures for cement plant—a review. *J. Clean. Prod.* **2015**, *103*, 260–274. [CrossRef]
15. Payá, J.; Monzó, J.; Borrachero, M.V.; Soriano, L.; Akasaki, J.L.; Tashima, M.M. New inorganic binders containing ashes from agricultural wastes. In *Sustainable and Nonconventional Construction Materials Using Inorganic Bonded Fiber Composites*; Elsevier: Amsterdam, The Netherlands, 2017; pp. 127–164. [CrossRef]
16. Alonso, M.; Gascó, C.; Morales, M.M.; Suárez-Navarro, J.; Zamorano, M.; Puertas, F. Olive biomass ash as an alternative activator in geopolymer formation: A study of strength, radiology and leaching behaviour. *Cem. Concr. Compos.* **2019**, *104*, 103384. [CrossRef]
17. Font, A.; Soriano, L.; de Moraes Pinheiro, S.M.; Tashima, M.M.; Monzó, J.; Borrachero, M.V.; Payá, J. Design and properties of 100% waste-based ternary alkali-activated mortars: Blast furnace slag, olive-stone biomass ash and rice husk ash. *J. Clean. Prod.* **2020**, *243*, 118568. [CrossRef]
18. Bernal, S.; Rodríguez, E.; Mejía de Gutiérrez, R.; Provis, J.L. Performance at high temperature of alkali-activated slag pastes produced with silica fume and rice husk ash based activators. *Mater. Constr.* **2015**, *65*. [CrossRef]
19. Peys, A.; Rahier, H.; Pontikes, Y. Potassium-rich biomass ashes as activators in metakaolin-based inorganic polymers. *Appl. Clay Sci.* **2016**, *119*, 401–409. [CrossRef]
20. Moraes, J.; Font, A.; Soriano, L.; Akasaki, J.; Tashima, M.; Monzó, J.; Borrachero, M.; Payá, J. New use of sugar cane straw ash in alkali-activated materials: A silica source for the preparation of the alkaline activator. *Constr. Build. Mater.* **2018**, *171*, 611–621. [CrossRef]
21. Alex, T.; Kalinkin, A.; Nath, S.; Gurevich, B.; Kalinkina, E.; Tyukavkina, V.; Kumar, S. Utilization of zinc slag through geopolymerization: Influence of milling atmosphere. *Int. J. Miner. Process.* **2013**, *123*, 102–107. [CrossRef]
22. Zhang, Z.; Zhu, Y.; Yang, T.; Li, L.; Zhu, H.; Wang, H. Conversion of local industrial wastes into greener cement through geopolymer technology: A case study of high-magnesium nickel slag. *J. Clean. Prod.* **2017**, *141*, 463–471. [CrossRef]
23. Ahmari, S.; Parameswaran, K.; Zhang, L. Alkali activation of copper mine tailings and low-calcium flash-furnace copper smelter slag. *J. Mater. Civ. Eng.* **2014**, *27*, 04014193. [CrossRef]